2015 International Symposium on Nonlinear Theory and its Applications
NOLTA2015, Kowloon, Hong Kong, China, December 1-4, 2015

How Short-Term Synaptic Depression Reshapes Dynamics of Continuous Attractor Neural Networks

He Wang†, Kin Lam†, C. C. Alan Fung†, K. Y. Michael Wong†, and Si Wu‡

†Department of Physics, Hong Kong University of Science and Technology,
Hong Kong SAR, P. R. China
‡State Key Laboratory of Cognitive Neuroscience and Learning,
IDG/McGovern Institute for Brain Research,
Beijing Normal University, Beijing 100875, P. R. China
Email: hwangaa@ust.hk, alan90312@gmail.com, fccaa33@gmail.com, phkywong@ust.hk, wusi@bnu.edu.cn

Abstract—The neural representation of spatially continuous information such as orientation, head direction, and spatial location is widely modeled as population activities in continuous attractor neural networks (CANNs). We investigate how short-term synaptic depression (STD) can reshape the intrinsic dynamics of the CANN model and its responses to external inputs. We find that weak STD enhances the mobility of population activities, while strong STD induces population spikes. Other complex behaviors may have the potential to provide a repertoire of dynamical representations in the neural system.

1. Introduction

To understand how information is encoded in the brain, it is crucial to consider the range of firing patterns and their conditions of occurrence [1]. In the processing of continuous information such as object orientation and spatial location, firing patterns are found to be localized in the space of preferred stimuli of the neurons, normally taking up a Gaussian-like profile [2, 3]. Thus an interesting question is whether these profiles are stable in time and in space and, if not, what other dynamical states will replace them.

In neural field models processing continuous information, Gaussian-like tuning curves are steady states of the network dynamics, and remain stable when their positions are displaced in the space of the preferred stimuli of the neurons. These neural field models are called continuous attractor neural networks (CANNs). The ability to support these Gaussian-like bump attractors is effected by couplings between neurons in CANNs. However, in reality, couplings between neurons are not quenched. They depend on firing histories of presynaptic neurons. Tsodyks *et al.* found that synaptic efficacy decreases with firing history [4, 5]. Furthermore, they proposed that this decline in synaptic efficacy is due to the slow dynamics of the recovery process of neurotransmitters. The recovery of neurotransmitters is of the order of 100 ms. This short-term decline in synaptic efficacy is called short-term synaptic depression (STD).

2. Intrinsic behaviors

N neurons are evenly distributed in the space of preferred stimuli (in the following simulation results, $N = 256$). Neurons are labeled by their preferred stimulus x. The range of $\{x\}$ is $(-L/2, L/2]$. So the size of the space is L. Since usually the model is applied to the representation of directions or orientations, $L = 2\pi$ and the periodic boundary condition is imposed. We modify the general form of neural field theory and formulate the intrinsic dynamics of the neuronal input $U(x,t)$ as [6, 2, 7, 8]

$$\tau_s \frac{\partial U(x,t)}{\partial t} = \int_{-L/2}^{L/2} dx' J(x,x') p(x',t) r(x',t) - U(x,t) + I(x,t), \quad (1)$$

where τ_s is the synaptic time constant, $I(x,t)$ is the external stimulus, $J(x,x')$ is the coupling strength between neurons with preferred stimuli x and x', and $r(x',t)$ is the firing rate of neuron x' at time t. They are given by

$$J(x,x') = \frac{1}{\sqrt{2\pi}a} \exp\Big(-\frac{\|x-x'\|^2}{2a^2}\Big), \quad (2)$$

$$r(x,t) = \frac{[U(x,t)]_+^2}{1 + \frac{k}{8\sqrt{2\pi}a}\int dx' [U(x',t)]_+^2}. \quad (3)$$

where k is the strength of the global inhibition, $[X]_+ \equiv \max(X, 0)$ and $\|X\| \equiv \min(|X|, L - |X|)$. Here we adopt a Gaussian coupling and incorporate inhibitory connections into the global inhibition.

$p(x,t)$ is the availability of neurotransmitters in neuron x. The dynamics of $p(x,t)$ is given by

$$\tau_d \frac{\partial p(x,t)}{\partial t} = 1 - p(x,t) - \beta p(x,t) r(x,t), \quad (4)$$

where τ_d is the time scale of neurotransmitter recovery, which is chosen to be $\tau_d = 50\tau_s$. β is the fraction of total neurotransmitters consumed by firing per spike.

In the absence of external inputs ($I(x,t) = 0$), a variety of interesting behaviors have been discovered, such as the static bump, the moving bump and the silent state

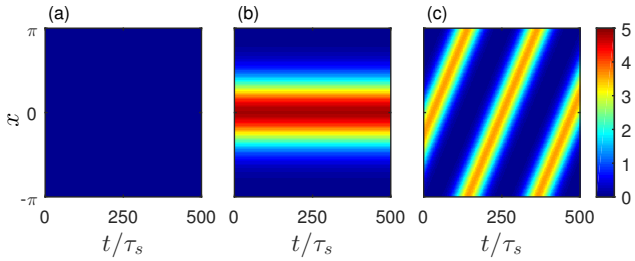

Figure 1: Intrinsic Behaviors. The color scale shows $U(x,t)$. (a) Silent state. Parameters: $k = 0.8, \beta = 0.2$. (b) Static bump. Parameters: $k = 0.8, \beta = 0.005$. (c) Moving bump. Parameters: $k = 0.8, \beta = 0.05$. For all (a)-(c), $a = 0.6$.

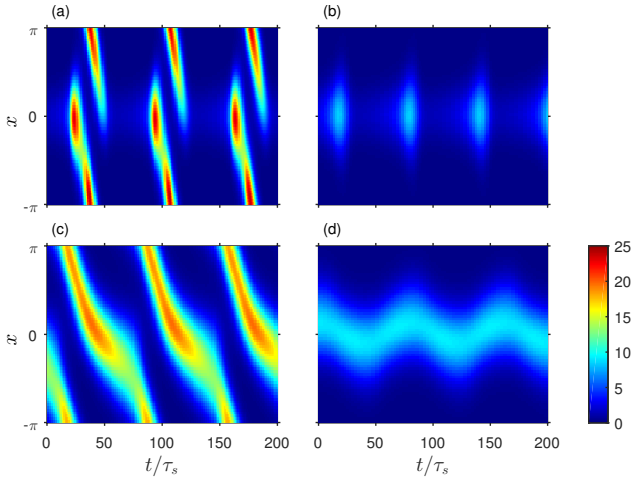

Figure 2: Four basic dynamic responses to a single static input in CANN with STD. The color (gray) scale shows the firing rate $r(x,t)$. (a) Emitter. Parameters: $k = 0.2, \beta = 0.3$. (b) Population spikes. Parameters: $k = 0.3, \beta = 0.4$. (c) Moving bump. Parameters: $k = 0.3, \beta = 0.1$. (d) Slosher. Parameters: $k = 0.5, \beta = 0.1$. For all (a)-(d), $A = 0.8$, $a = a_A = 48^\circ = 0.8378$.

(Fig. 1(a)-(c), see also [8]). The static bump state, also known as a persistent spatially localized activity state [9], is of interest because it can be found in physiological recordings in the prefrontal cortex during spatial working memory tasks and other systems that encode directional or spatial information. The moving bump state corresponds to traveling waves which have been extensively studied experimentally [10, 11, 12] and theoretically [13, 14, 15, 16, 17]. In our model, neurotransmitters are depleted at the bump's position due to the STD. Thus, the bump tends to move away to regions where neurotransmitters are more available.

3. Responses to a single static input

In this section, we will discuss the network behavior in the presence of a single static input and moderate global inhibition. For the external input in Eq. (1), we adopt the form $I(x,t) = A\exp[-(x-z)^2/(2a_A^2)]$, where z is the center of that input (without loss of generality, $z = 0$ in this work), A is the strength of the input, and a_A is the width of the input. Note that the behavior of this system is controlled by three parameters, namely the strength of the global inhibition k, the strength of the STD β and the strength of the external input A. In this work, different response patterns are discussed in the parameter space spanned by these three quantities.

3.1. Four Basic Dynamic Response Patterns

The static bump is expected to be the simplest form of response. However, in a very large region of the parameter space, static bumps are unstable and much more interesting response patterns emerge. Among them, there are four basic dynamic patterns through which we can understand the general property of this system (Fig. 2(a)-(d)).

One response pattern is the moving bump. Moving bumps result from the mobility of the neural field enhanced by the STD. Once a bump is built, neurotransmitters are depleted in the bump region, leading to a tendency of the bump to move away to fresher regions. As an intrinsic behavior, the moving bump will keep its profile and its speed all the time (Fig. 1(c)). However, while the static input is imposed, the speed and profile of the bump will change when the bump crosses the input. The bump is higher and faster when approaching to the input, while weaker and slower when leaving the input, because the external input tends to attract the bump (Fig. 2(c)).

When the attraction provided by the external input is strong and the mobility enhanced by the STD is not sufficient for the bump to overcome the attraction of the input, the bump gets trapped and moves side-to-side around the external input. It is called a slosher (Fig. 2(d)) [18].

In both cases of the moving bump and the slosher, the dynamics are governed by the mobility enhanced by the STD and the attraction provided by the external input. The amplitude of the bump does not change significantly during its movement. However, when β and A are sufficiently large, the effect of the STD is not just mobility enhancement, but also amplitude modulation. Large β and A means that the bump will consume more neurotransmitters so that it cannot maintain its amplitude all the time. The emitter (Fig. 2(a)) is an example in such case. One moving bump is emitted by the external input. After it travels around the network, the bump dies down due to the excessive consumption of neurotransmitters during traveling. Then, the network waits a while until sufficient amount of neurotransmitters is recovered to support another emission of the moving bump. When the external input is even stronger, we see a similar response, namely, population spikes (Fig. 2(b)), in which case a static bump, rather than a branch of moving bump, is emitted after recovery, since the external input is so strong that the bump is trapped [19, 20].

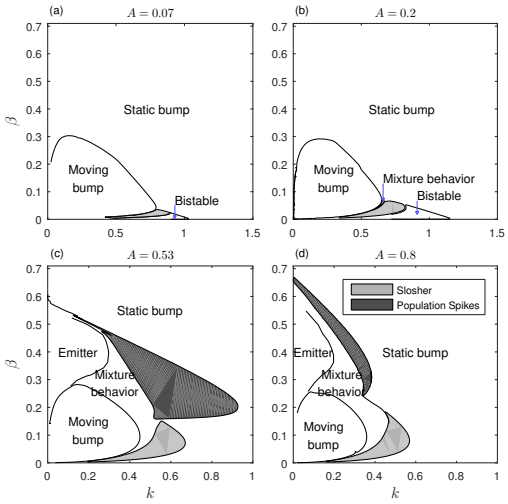

Figure 3: Phase diagrams for the four basic responses in the space of k and β with different values of A. $a = 0.5$ and $a_A = \sqrt{2}/2$.

We explore the four basic dynamic responses in the parameter space of k and β with different values of A (Fig. 3). When the input is weak (Fig. 3(a) and (b)), sloshers appear between the moving bump region and the static bump region. This is because the mobility enhanced by the STD is not enough to delocalize the bump, which is attracted by the static input. When the input is strong (Fig. 3(c) and (d)), the consumption of neurotransmitters is so fast that the bump cannot keep its amplitude stable. This results in the emergence of the emitter and population spikes.

3.2. Mixture Behaviors

In numerical solutions, we find that in a large part of the parameter space, response patterns can be none of the four basic patterns and very complex. They seem to be different mixtures of the four basic dynamic patterns. Relations between different mixture behaviors can be understood systematically by monitoring the period of asymptotic states. Thus, we can show how different mixture behaviors are organized in the phase diagram (Figs. 4).

For the full model simulation (Fig. 4), where the number of neurons is 256, Eqs. (1)-(4) are solved by using the MATLAB command ode45 and the period is determined by examining the auto-correlation function of asymptotic states.

In the phase diagram, there are many patches within which the period of the dynamics changes continuously. However, the period jumps abruptly across boundaries of the patches. This indicates that behaviors are similar within each patch, while transitions happen across boundaries. In the gray region along phase boundaries, different dynamics can be found by starting with initial conditions from different sides of the boundaries. The four basic dynamic response patterns are located at the four disjoint regions of the phase diagram. In between them, there is a rich spectrum of different mixture behaviors. Especially, black dots, where the length of the period is too long to be well determined within a time limit, are found in the mixture behavior region, which may imply chaos. Largest Lyapunov exponents are computed in regions containing black dots (Fig. 5). Positive exponents exist extensively around $\beta = 0.2$, which clearly demonstrates the existence of chaos in this strongly coupled neural field.

Having explored the phase diagrams in different situations, we find that the parameter space can be separated into two parts. The upper part where β is larger consists of emitters, population spikes and their mixtures. The lower part where β is smaller consists of moving bumps, sloshers and their mixtures. Between these two parts around $\beta = 0.2$, responses tend to have very long period and show chaotic features. We may conclude that short-term synaptic depression have different effects depending on its strength.

Weak STD enhances the mobility of the bump without affecting the amplitude of the bump significantly, leading to bumps of relatively stable amplitude and varying position. This is the spatial modulation effect of the STD. On the other hand, strong STD disrupts the bump in time, since neurotransmitters are depleted rapidly during the spikes. This shows the temporal modulation effect of the STD. Bumps in the time sequence generally are not the same, implying a possibility to encode different information in different emissions, an example having been discussed in detail in [21].

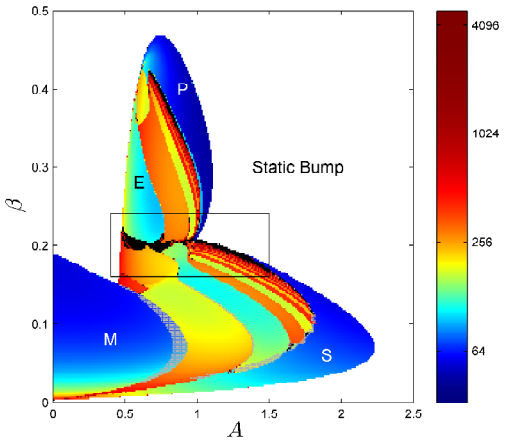

Figure 4: Phase diagram in the space of A and β. The color scale indicates lengths of the periods in log scale. Black dots mean the period of the response is longer than $5000\tau_s$. The global inhibition strength $k = 0.3$. $a = a_A = 0.8378$. M, E, P and S represent "moving bump", "emitter", "population spikes" and "slosher", respectively. The gray regions are bistable regions where the lengths of the periods can be either of two different values. The box encircles the region where largest Lyapunov exponents are computed and shown in Fig. 5.

4. Discussion

We have found that the STD enriches the responses of the CANN model in the presence of a single static input, including four basic patterns of dynamic responses and their mixtures. When STD is weak (lower than 0.2, roughly), it mainly provides spatial modulation, or in other words, enhances the mobility of the bump. Inputs of different strengths provide different attraction, leading to moving bumps, sloshers or mixtures of them. When STD is strong, STD provides temporal modulation along with spatial modulation. Together with the static external input, they results in emitters, population spikes, or mixtures of them. Detailed examples of mixture behaviors can be found in [23]. In the parameter region where STD strength is intermediate, chaotic behaviors appear. Although it is not fully understood, we believe that the involvement of both temporal and spatial modulation of STD is the major cause of complexity in that region.

Our work shows that even a recurrent network with a highly regular structure can support extremely complex dynamics and chaos, in the presence of short-term synaptic plasticity. A rich spectrum of dynamical behaviors can be readily found and understood near the edge of chaos. How to tap into the potential computational power of CANNs with STD is an interesting problem to be investigated in the future.

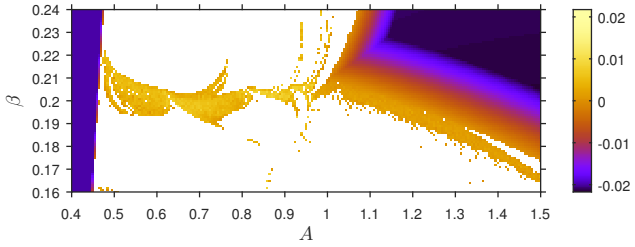

Figure 5: Largest Lyapunov exponents (LLE). The blank region contains periodic behaviors. Parameters are the same as those in Fig. 4.

Acknowledgments

This work is supported by the Research Grants Council of Hong Kong (grant numbers 604512, 605813 and N_HKUST606/12), National Basic Research Program of China (2014CB846101) and the National Natural Science Foundation of China (31261160495).

References

[1] D. J. Amit, "Modeling Brain Function: The World of Attractor Neural Networks," Cambridge University Press, 1992.

[2] S. Amari, *Biol. Cybern.*, vol.27, pp.77, 1977.

[3] R. Ben-Yishai, R. L. Bar-Or, and H. Sompolinsky, *Proc. Natl. Acad. Sci. USA*, vol.92, pp.3844, 1995.

[4] M. V. Tsodyks and H. Markram, *Proc. Natl. Acad. Sci. USA*, vol.94, pp.719, 1997.

[5] M. Tsodyks, K. Pawelzik, and H. Markram, *Neural Comput.*, vol.10, pp.821, 1998.

[6] H. R. Wilson and J. D. Cowan, *Biophys. J.*, vol.12, pp.1, 1972.

[7] C. C. A. Fung, K. Y. M. Wong, and S. Wu, *Neural Comput.*, vol.22, pp.752, 2010.

[8] C. C. A. Fung, K. Y. M. Wong, and S. Wu, *Advances in Neural Information Processing Systems 25*, pp.1097, 2012.

[9] M. Camperi and X. J. Wang, *J. Comput. Neurosci.*, vol.5, pp.383, 1998.

[10] R. Chervin, P. Pierce, and B. Connors, *J. Neurophysiol.*, vol.60, pp.1695, 1988.

[11] D. J. Pinto, S. L. Patrick, W. C. Huang, and B. W. Connors, *J. Neurosci.*, vol.25, pp.8131, 2005.

[12] K. A. Richardson, S. J. Schiff, and B. J. Gluckman, *Phys. Rev. Lett.*, vol.94, pp.028103, 2005.

[13] D. Golomb and Y. Amitai, *J. Neurophysiol.*, vol.78, pp.1199, 1997.

[14] G. B. Ermentrout and D. Kleinfeld, *Neuron*, vol.29, pp.33, 2001.

[15] D. J. Pinto and G. B. Ermentrout, *SIAM J. Appl. Math.*, vol.62, pp.206, 2001.

[16] P. C. Bressloff and S. E. Folias, *SIAM J. Appl. Math.*, vol.65, pp.131, 2004.

[17] S. Coombes and M. R. Owen, *SIAM J. Appl. Dyn. Syst.*, vol.3, pp.574, 2004.

[18] S. E. Folias, *SIAM J. Appl. Dyn. Syst.*, vol.10, pp.744, 2011.

[19] A. Loebel and M. Tsodyks, *J. Comput. Neurosci.*, vol.13, pp.111, 2002.

[20] S. Mark and M. Tsodyks, *Front. Comput. Neurosci.*, vol.6, pp.43, 2012.

[21] C. C. A. Fung, H. Wang, K. Lam, K. Y. M. Wong, and S. Wu, *Front. Comput. Neurosci.*, vol.7, pp.73, 2013.

[22] S. Treue, K. Hol, and H. Rauber, *Nat. Neurosci.*, vol.3, pp.270, 2000.

[23] H. Wang, K. Lam, C. C. A. Fung, K. Y. M. Wong, and S. Wu, *Phys. Rev. E*, accepted, 2015.